https://doi.org/10.2352/EI.2023.35.15.COLOR-183

Intraocular Glare affects Lightness Illusions

John J. McCann; McCann Imaging; Arlington, MA 02474 USA

Abstract

Lightness Illusions (Contrast, Assimilation, and Natural Scenes with Edges and Gradients) show that Lightness appearances do not correlate with the light sent from the scene to the eye. Illusions modify "the-rest-of-the-scene" to make two identical-luminance Gray segments appear different from each other. Scene segments have two properties in human vision: apparent Lightness, and apparent Uniformity. Models of vision have two scene-dependent processes that spatially transform scene luminances. The first is optical veiling glare that modifies the sharpness of the edges, and replaces uniform scene segments with low-slope gradients. The second scene-dependent transformation is neural spatial processing. This means that this spatial transformation has many tasks to perform in generating appearances. They include: making edges appear sharp; making gradients in scene segments appear uniform; and compensating for glare's many local redistributions of light. In short, neural spatial processing does an excellent job of ignoring glare's distortions of scene luminance. In fact it over compensates glare in a way that generates appearances reported in Contrast Illusions, B&W Mondrians, and Checkershadow Illusions.

Introduction

Lightness Illusions proved a long time ago that human vision is a *scene-dependent* process; that is, the appearance of scene segments responds to the content of the entire scene. There are alternative scientific models based on *scene-independent radiances* from single scene-segments, such as silver-halide films' responses to light, the quanta catch of visual pigment molecules, and colorimetry. These single segment models can predict films responses, but cannot predict human appearances. Colorimetry can predict color matches of two stimuli in a no-light surround. However, they cannot predict the color appearance of those two color-matched stimuli. (1) These single-segment models cannot model human spatial vision's response to complex scenes. Visual illusions have proved that the "rest-of-the-scene matters.

Figure 1 shows both Contrast and Assimilation Lightness Illusions. These visual targets are restricted to three scene-luminance components: White, Gray, and Black.

Contrast's Gray Regions of Interest (GrayROI) are the two large Gray rectangles in the top-left large White surround, and the top-right large Black surround. The Gray-in-White ROI appears darker than the Gray-in-Black ROI. Both ROI appear uniform.

Assimilation's GrayROI are the two pairs of 3 Gray stripes in alternating White and Black stripes. The Gray-between-White stripes (bottom-left) ROI appears lighter than the Gray-between-Black stripes ROI (bottom-right). All four GrayROIs appear uniform.

Lightness Illusions' placement of Black and White patterns changes Grays appearances to be *scene-content* specific. Observe in Contrast that the top-left *Gray-in-White* appears darker than top-right. Then, observe in Assimilation that the bottom-left Gray-in-White appears lighter in striped surround than Gray-in-Black(bottom-right). These <u>different</u> Gray appearances are the result of the scene's spatial content, and spatial arrangements of segments made from uniform Whites and Blacks.

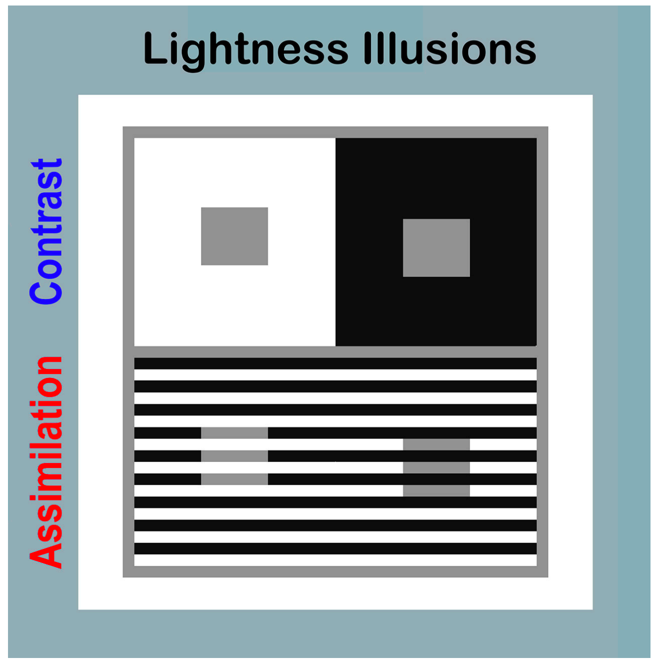

Figure 1 shows the combination of a Contrast Illusion (top); and Assimilation Illusion (bottom). All Whites have constant uniform luminance of 450 cd/m². Grays and Blacks have uniform luminances of 136; and 2.24 cd/m² viewed on a XDR display. The combined Illusion subtends 10° square. The Lightness Illusions have a range of luminance of [1, 200], that is a range of log luminance of [0.0, 2.3].

ROI-Grays' appearances are the consequence of two spatial properties of the scene. First, the scene's histogram, describing populations of all scene pixels (independent of location). Second, size, shape, and location of White and Black segments. In other words, the arrangements of the spatial content in the "rest-of-the-scene" modifies the appearances of GrayROI equal scene luminances.

Contrast+Assimilation Illusions are robust. Contrast is insensitive to target size (or viewing distance) that changes retinal size.(2) Changing viewing distance alters spatial-frequency distribution (intensity vs. cycles/degree). As well, Contrast+Assimilation are insensitive to varying luminance levels. Viewing them in conditions that excite only rods generates the same spatial effects; they just appear dimmer. Viewing color Contrast+Assimilation Illusions in conditions that excite only rods and long-wave cones generates the same color spatial effects, they just appear different hues, and less-sharp than in photopic vision. (3,4)

Optical Veiling Glare

Our visual system transforms scene-luminance patterns using two independent spatial mechanisms: optical, then neural. First, optical veiling glare transforms scene luminances into a different light pattern on receptors. Equal scene luminances become unequal retinal luminances. Uniform scene segments become nonuniform retinal gradients. The scene's darker segments acquire substantial scattered light; and that alters the range of light on the retina compared with the scene's range.

Glare responds to the content of the entire scene. The glare on each receptor is the sum of the individual contributions from every other scene segment. Glare is a *scene-dependent* optical transformation.

After glare the pattern of light on receptors is a morass of high- and low-slope gradients. Quantitative measurements, and pseudocolor renderings are needed to appreciate the magnitude, and spatial patterns of glare. Glare's gradients are invisible when you inspect them. Illusions are generated by neural responses from "the-rest-of-the-scene". The neural network input is the simultaneous array of all receptors' responses.

Neural processing performs vision's second scene-dependent spatial transformation. Neural processing generates appearances in Illusions and Natural Scenes. "Glare's Paradox" is that glare adds more re-distributed light to GrayROIs that appear darker, and less light to those that appear lighter. This article describes 5 experiments in which neural-spatial image processing overcompensates the effects of glare.

This article studies the first-step in imaging: scene-dependent glare. It shows glare's transformations of light sent from the scene to the eye with respect to both uniformity, and the equality of retinal luminances. This article reveals glare's modification of input data used in quantitative image analysis and models of vision. Glare redefines the challenges in modeling Lightness Illusions. Neural spatial processing is more powerful than we realized because of glare's transformation of the light on the retina.

Calculating the Retinal Image

We used a new open-source Python program (5) to transform the entire scene content (input luminance pattern) into the pattern of light on the retinal array of receptors.(6) The Python program that calculates glare's effects on Illusions has two parts. First, the Python program makes an array of calibrated display luminances and convolves it with Vos and van den Berg's (7) CIE 1999 Glare Spread Function (GSF) for human vision. Second, it displays pseudocolor visualizations of the millions of pixels in each scene, and its retinal image. These visualizations reveal the spatial contours of glare's subtle gradients. The article describes:

- CIE GSF used to calculate each pixel's contribution to a single distant pixel as a function of the angular separation between donor and receiving pixels
- Description of the GSF's of fall-off of glare with separations from source pixel
- The programs 64-bit double precision accumulation of all the tiny glare contributions from all pixels
- Fast Fourier Transform convolution of the entire scene with CIE 1999 GSF using image padding
- Analysis of the image on the retina using $\log_{10}$ images set to the input range of the scene
- Pseudocolor rendering of all 2048 by 2048 pixels to visualize the gradients in retinal luminance. (6)

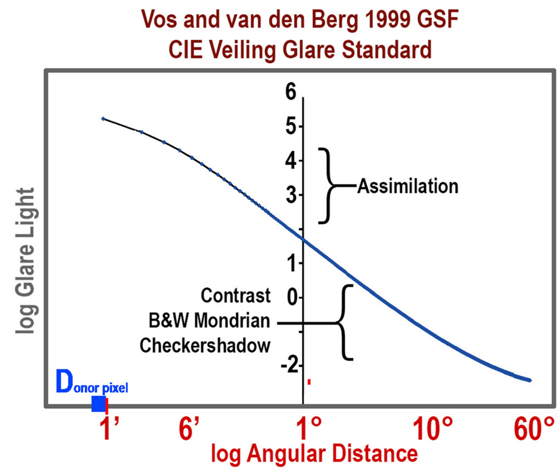

Figure 2 shows Vos and van den Berg's Glare Spread Function for human vision.

The CIE Glare Spread Function GSF is plotted on log-log axes in Figure 2. Note the extreme ranges of these axes. The horizontal *visual-angle axis* covers (1 minute to 60°). The vertical *Glare light axis* plots the decrease in glare as the function of the angular separation between donor pixel and receiving pixel. It covers 8 $\log_{10}$ units (150,000 to 0.005). Despite its range, it does not approach a constant asymptote. The glare on each receiving pixel is the unique sum of contributions from all the other scene pixels. Glare is a *scene-content-dependent* transformation of all scene luminances.

Glare's modification of Gray ROIs

Figure 3(left) shows the input scene of Contrast+Assimilation on the Apple XDR display. It is a close approximation of the image the author saw on his screen. The luminances from the author's screen was measured with a KM 100A meter. The python program used this data to make the linear luminance convolution array (2048 by2048 pixel). When this display was viewed at 24 inches, the scene subtended 10°; each pixel subtended 0.24 min of arc (slightly smaller than spacing of foveal cones).

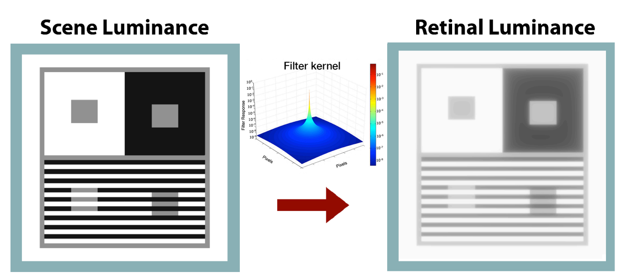

Figure 3(left). Scene on XDR display; Figure 3(right). Calculated image on the retina after convolution with Glare Spread Function kernel shown in center (above the arrow).

The 2D GSF convolution kernel is shown above the arrow in the center of Figure 3. The right side shows the calculated pattern of light on the retina. The information in the four megapixel, linear, 64-bit double precision, convolution cannot be rendered accurately on any display. We scaled the output to 8-bit $\log_{10}$ using the range of the input image [0.0, 2.3].

The standard practice for evaluating the results of image processing is to compare the input image on the left with the output image on the right. The input Contrast+Assimilation image has only White, Gray and Black pixels. These three pixel values were measured to have 450, 136, and 2.24 cd/m². These segments are uniform with a standard deviation of 0.0. Table 1 lists their luminance, log range, and their position in linear range [1, 200].

Pixels	Black	Gray	White
% All Pixels	29%	14%	57%
Luminance (cd/m²)	2.24 ±0	136 ±0	450 ±0
Log range	0	1.34	2.3
Position in range	1	58	200

Table 1. List of Scene luminance pixel statistics.

However, in the case of studying optical veiling glare, we have a problem. The above convolution redistributes the scene's luminances to make the image on Figure 3(right). When we inspect that image with our eyes we add more glare to our glare calculation. It is the numerical value of each pixel that is the important accurate data. Observing the appearances in the *retinal luminance* image just distorts the data. We also need to recall that Illusions prove that visual appearances do not correlate with luminances. Visual inspection of the calculated retinal image does not provide the information we want.

Evaluating Calculated Retinal Luminances

The study of Glare requires special image processing tools to analyze, and visualize the individual luminance values of the calculated retinal image. We need to use:

- Histograms to measure the distribution of retinal luminance pixel values in scene segments.
- Pseudocolor renditions to visualize the spatial patterns of light found in apparently uniform gradients.

Histograms Counts

The horizontal axis in Figure 4 plots the position in the linear range [1, 200] covering the scene's input luminances. Blacks are 1, Grays are 58, and Whites are 200. The vertical axis is the count of the number of pixels for each of 256 bins between 1 and 200.

GrayROI have identical scene luminance in A,B,C,D. Glare redistributed the light in the normalized retinal image. All segments showed a distribution of values indicating that these uniform segments with sharp edges were transformed into gradients. GrayROI-A has the narrowest distribution in Contrast's large Black surround. Contrast's GrayROI-B in its large White surround has a broader glare distribution. Remarkably, B appears darker than A despite the fact that all of their pixels have much more light than those in A. This is called Glare's Paradox, when after glare, image segments with more light appear darker, and segments with less light appear lighter.

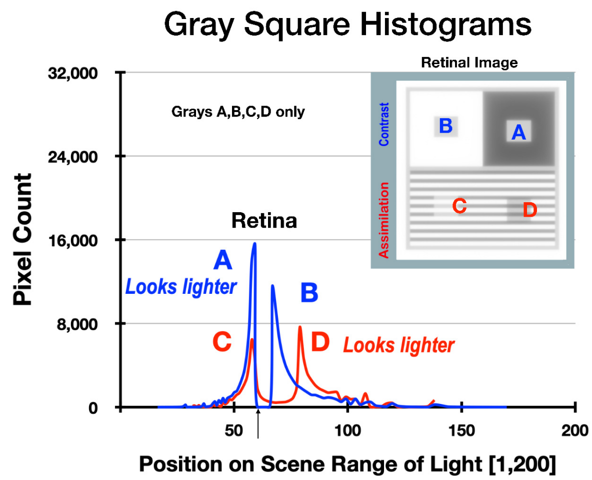

Figure 4. Histogram of GrayROI pixels in the calculated retinal luminance image. The retinal image is shown in the inset that identifies Contrast and Assimilation. Square A is Gray-in-White Contrast; B is Gray-in-Black Contrast; C is Gray-in-White Assimilation; D is Gray-in-Black Assimilation.

Michael White's Assimilation Illusion has fewer pixels in their C and D GrayROI segments because the background is made of stripes. GrayROI-D is three stripes with Black above and below, with White on their sides. Their histogram shape is very similar to that seen in Contrast's GrayROI-A, but with fewer pixels.

GrayROI-C is three stripes with White above and below it, with Black on their sides. Their retinal luminances are much higher than those of the other histograms. The shape of the distribution is much broader than the others.

Assimilation does not show Glare's paradox. GrayROI-C appears much lighter when its retinal luminances are much higher. GrayROI-D appear darker with lower retinal luminances.

The Contrast + Assimilation test target illustrates the little-studied properties of angular size and separation. Contrast has larger Grays, and much larger separations of Whites and Blacks. Assimilation has smaller grays with much smaller separations.

The plot of GSF in Figure 2 shows that glare falls off dramatically as a function of log angular subtend. Figure 2 show that a max-luminance pixel's contribution to a 0.1° separation neighbor is 550 times that of a 1.0° separation neighbor; and 300,000 times greater than a 10° separation neighbor.

We cannot judge the effects of glare without performing the GSF convolution with all the scene's pixels. All the pixel contributions matter. However, the separation of max-luminance pixels from Grays and Blacks has major consequences in each pixels contribution to glare in each scene segment. As well, the shape of each segment has major glare consequences. The brackets in Figure 2 indicate the regions of the GSF influences. They show that Assimilation smaller size and smaller separations result in higher glare contributions, than those of Contrast.

In summary, histograms of the GrayROI segments show that uniform scene luminances are transformed by glare into gradients in the pattern of light on the retina. However, when we study the appearances in Figure 1, all four segments appear uniform. This demonstrates that one of the roles of post-receptor neural spatial processing must be to transform substantial gradients of luminance into uniform image segment appearances.

While histograms allow us to measure the ranges of non-uniformities it cannot describe the pattern of light caused by glare's transformations.

Pseudocolor Visualizations

Many glare-generated gradients in calculated retinal luminance patterns are invisible in grayscale renditions. Human vision's spatial-image processing suppresses the visibility of luminance gradients. (11)

The experiment present here show that glare transformed all discontinuous sharp edges into steep retinal gradients. Many low-slope gradients are below human detection threshold. Visual inspection of retinal luminance does not reveal these gradients.

Pseudocolor maps, with visible quantization steps, converts subtle luminance gradients into discriminable bands of color, allowing readers to visualize the patterns of bands of equal-luminance regions, that reveal glare's nonuniform luminance transformations.

<cmap.LUT>

Figure 5 shows a Pseudocolor LookUp Table (LUT) called <cmap.LUT> that is used in the Python code. It divides the 256 levels in 8-bit data into 32 uniform bands, 8 digits wide. The sequence of the 32 different colors emphasizes the changes in appearance from White to Black.

This 3-3-2 RGB.LUT. is part of the ImageJ open source library.(8) This Pseudocolor LUT uses its 256 color bands to emphasize contours. This LUT assigns a different color to each segment made up of the same digit value over the range [0,255]. Recall the appearance of these White, Gray, and Black segment in Figure 1. This figure visualizes clearly the departures from uniformity introduced by optical veiling glare. These image transformations reveal the post-receptor neural spatial processing.

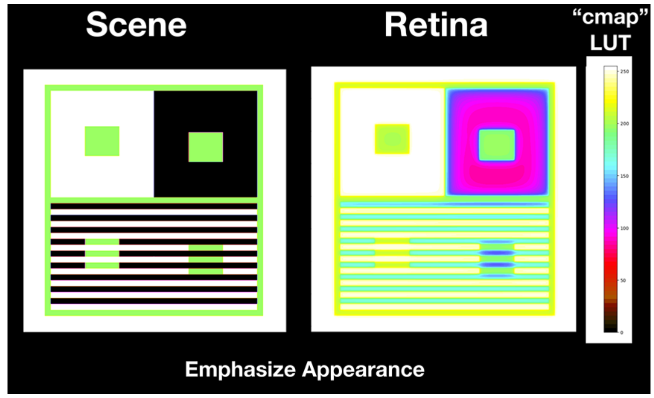

Figure 5. Scene and Retina luminances rendered by <cmap.LUT>. Figure 5(right edge) maps all 32 uniform color bands to visualize the digital values from 0 to 255. Figure 5(left) identifies that White scene segment have digital ranges from 247 to 255; Black segments have digital ranges from 0 to 8. Since the input and output images has been scaled to $\log_{10}$ normalized luminance, White to Black range is scaled to log range [0, 2.3]. Figure 5(Retina) shows the changes in GrayROI by different bands of color. More important is the visualizations of spatial information. In particular, the erosion of edges, and the distortions of straight lines are apparent.

<3-3-2 RGB.LUT>

Figure 6 show a Pseudocolor LUT with 256 distinct bands of color called <3-3-2RGB.LUT>. It is part of the ImageJ open source library.(9) This Pseudocolor LUT uses its 256 color bands to emphasize contours.

Pseudocolor rendering makes the spatial patterns of these gradients highly visible. Pseudocolor renditions visualize the spatial-image processing of post-receptor neurons.

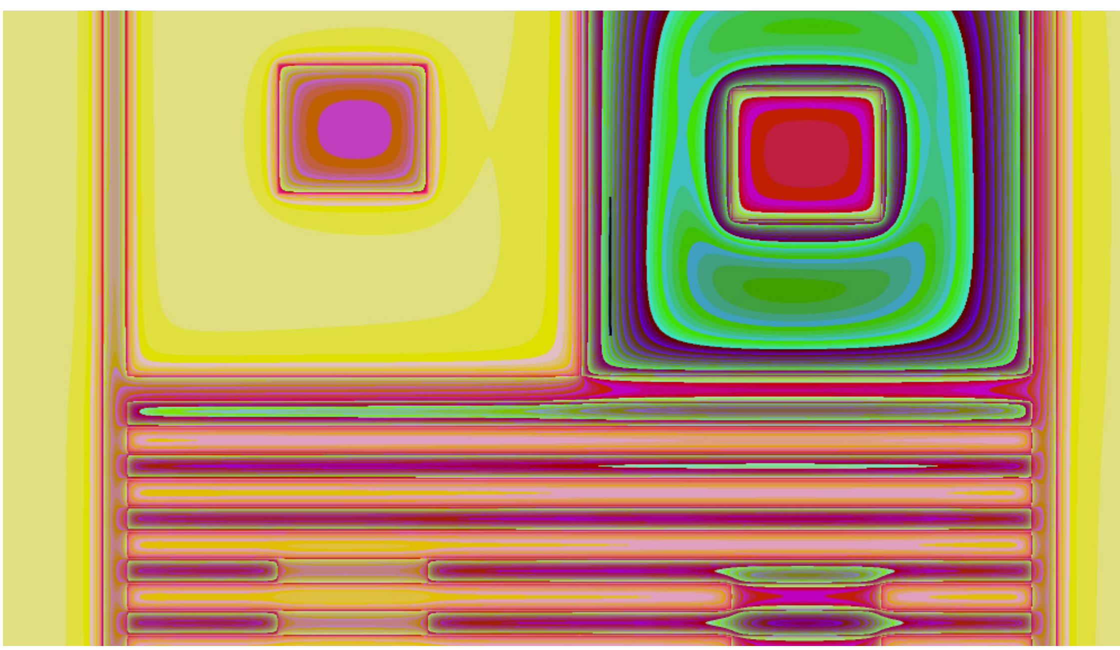

Figure 6. Magnified section of retinal luminance output image rendered by <3-3-2 RGB.LUT>. This LUT assigns a different color to each segment made up of the same digit value over the range [0,255]. Recall the appearance of these White, Gray, and Black segment in Figure 1. This figure visualizes clearly the departures from uniformity introduced by optical veiling glare. These image transformations reveal the post-receptor neural spatial processing required to synthesize the appearance of uniform White, Gray, and Blacks in Figure 1.

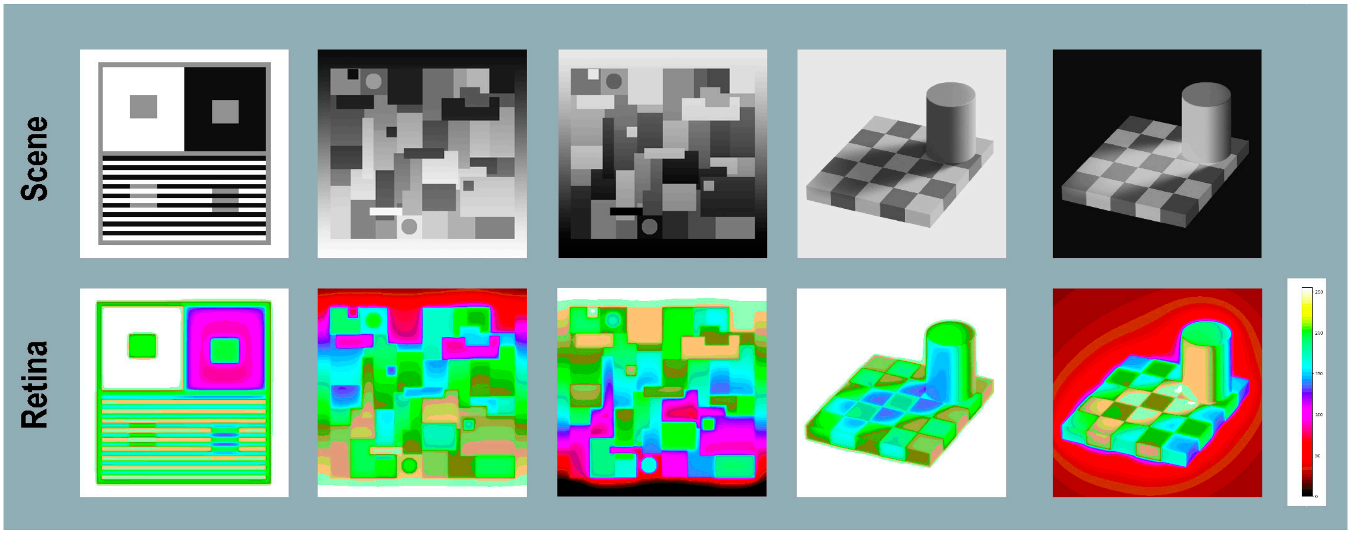

Figure 7 Glare's Paradox-Scene: (top-row) shows Appearances of : Contrast, positive and negative Mondrians and Checkershadows. Retina:(bottom-row) pseudocolor rendering using [cmap.LUT]. On the far right is a plot retinal contrast digit value [0,255] vs. pseudocolor samples used to identify retinal luminance values. All 5 scenes contained GrayROI segments that showed Glare's Paradox. Only the Assimilation Illusion does not show Glare's Paradox. Figure 7(right edge) maps all 32 uniform color bands to visualize the digital values The input and output images have been scaled to log range [0, 2.3]. Figure 5(Retina) shows the changes in GrayROI by different bands of color.

Glares Paradox

Figure 7(top) shows the appearance of Contrast, Edwin Land's B&W Mondrian, and Ted Adelson's Checkershadow computer display. It includes Negative displays of Mondrian and Checkershadow made with (Photoshop's® Invert function). Negative versions work very well. The Mondrian has a different pattern with top-illumination. The "shadow" in Checkershadow now appears to emit light.

Figure 7 (bottom-row) shows the calculated retinal luminances rendered by pseudocolor *<cmap.LUT>*.(6) The Contrast + Assimilation Illusion has been described above in this article with histograms and Pseudocolor.

Figure 8 describes the result of numerical analysis of the pairs of ROIs in Mondrian circles and Checkershadow squares. Figure 8 simply lists the mean value of each pair. These ROI means are shown on the same scale used in Figure 4, namely "The Position on the Scene Range of Light [1 , 200]".

Glare's Paradox				
Mean value [1,200] range				
darker ROI	**99**	**59**	**68**	**103**
lighter ROI	**79**	**41**	**56**	**115**

Figure 8. List of mean values of the 4 pairs of ROI with equal scene luminances. All pairs exhibit Glare's Paradox, namely every segment that appears lighter has lower retinal luminances. Every ROI that appears darker has higher retinal luminances.

These Illusion targets (Contrast; Positive- and Negative-Mondrians and Checkershadows are all examples of *Glare's Paradox*. Namely, darker GrayROIs appearances have more glare light. These darker ROIs are in local regions with higher-than-average *scene_luminances.* The sequence of observations is:

- greater average *scene luminance* region➞
  - greater glare➞smaller edge ratios➞
    - higher-slope visual response function➞
      - darker appearance].

Glare's Paradox exhibits reciprocal properties for GrayROIs that appear lighter. In all Contrast and Natural Scene examples: the sequence of observations is:

- lower average *scene_luminance* regions➞
  - less glare➞
    - larger edge ratios➞
      - lower-slope visual response function➞
        - lighter appearance].

Glare's Paradox is not found in Assimilation segments. Glare adds more glare to segments that appear lighter; less light to segments that appear darker. The angular separation between max and min are smaller, and local *retinal luminance* range is smaller. Glare assists Assimilation's change in appearance.

Discussion

There are four different strands of vision research that can be spun together to make a stronger story. The first is human vision response to High-Dynamic-Range(HDR) scenes. Glare determines the range of light that falls on the retina. Glare set both the global range and the local patterns of light.

HDR

Published work showed large reductions of retinal-dynamic range in maximal-glare scenes. Two transparent films were superimposed to make 40 patches (white-to-black) with scene luminance range of 5.4 log units. All patches were surrounded by a max-luminance surround. After intraocular glare the retinal contrast range was 1.5 log units. In a nearly million:1 range scene, glare reduced the range of light on the retina to 33:1. The scene's appearance varied from bright-white to very-dark black.(9)

A second experiment changed the background around each of the 40 patches from max-luminance to min-luminance. In this nearly million:1 range scene, glare reduced the range of light on the retina to 5,000:1. The second scene's appearance also varied from bright-white to very-dark black. Observers reported that whites appeared the same white in both experiments. Remarkably, blacks appeared the same black in both experiments despite the change in range from 33:1 to 5,000:1. (9)

Appearances over the range of white to black have variable scene-dependent response functions to light on receptors. In all cases, these response functions are all straight-line log luminance plots, with variable, scene-dependent slopes. (9,10)

LDR

The second strand is the present experiments on Low-Dynamic Range illusions. The magnitudes of glare contributions tracks the extreme change from million:1 range down to the present 200:1. Nevertheless the principles are the same. The Lightness Illusion introduced two new design features. First, all scene elements were perfectly uniform. Second, the entire surround was limited to only white (maximum source of glare), and Blacks (most affected by glare).

Glare's Paradox

The third strand is Glare's Paradox. Receptor responses after glare are inconsistent with the fundamental idea that more light looks lighter. Post-receptor neural spatial processing renders appearances of Contrast Illusions, and other examples of Glare's Paradox such that that more light appears darker, and less light appears lighter.

Glare's is hard to see

The fourth strand is the gradients of scene luminance are hard to see. Some times gradient are invisible, other time just detectable, or noticeable. Gradients are never as visible as edges with the same change in luminance.(11)

These four threads are consistent in that they demonstrate that there is no fixed "response function" of the eye. The Weber -Fechner Laws describe detection but are uncorrelated with the appearances of scene segments in HDR, LDR, Lightness Illusions, and Glare's paradox. Vision in the Natural World is scene dependent. Appearances are built up from edges, and gradients are processed to make them "hard to see". The practical consequence is that our vision does an excellent job of ignoring glare, so as to gather more visual information. Our visual system is indifferent to the task of reporting the scene's patterns of light on retinal receptors. Those pattern are degraded by glare, and that limits the information we need.

Successful models of vision need to mimic the eye's ability to ignore glare.

Acknowledgements

This work is the collaboration with Vassilios Vonikakis, Alessandro Rizzi with major contributions from T. van den Berg, J. Coppens, I. Farup, W. A. Stiehl, R. Savoy, J. Frankle; and Mary McCann for her thoughtful discussions.

References

(1) J.J. McCann, "What scene information is needed for models of color appearance in the natural world?), Color. Technol. 137, 5–15, (2020). doi: 10.1111/cote.12502

(2) J.J. McCann, "Visibility of gradients and low-spatial frequency sinusoids: evidence for a distance Constancy mechanism", J. Photogr. Sci.Eng. 22, 64–68, (1978)

(3) J.J. McCann, (2012). "Color assimilation and contrast near absolute threshold", Proc. SPIE 8292, Color Imaging XVII: Displaying, Processing, Hardcopy, and Applications, 829203 (24 January 2012) ; doi: 10.1117/12.912003

(4) J.J. McCann, (2021c). Rod-Lcone. Available at: https://www.retinex2.net/Publications/rod-lcone.html (Accessed Jan 30, 2023).

(5) V. Vonikakis, (2022). Github citation: bbonik/retinal-contrast-glare. Available at: https://github.com/bbonik/retinal-contrast-glare (Accessed Jan 30, 2023).

(6) J.J. McCann, V. Vonikakis, and A. Rizzi, "Edges-and Gradients in Lightness Illusions: Role of Optical Veiling Glare" Front. Psychol., 15 December 2022, Sec. Perception Science, Volume 13 2022 | https://doi.org/10.3389/fpsyg.2022.958787

(7) J.J. Vos and T.J.T.P van den Berg, "Report on Disability Glare", CIE Collection 135, 1–9, (1999).

(8) (NIH) National Institute of Health ." ImageJ® - Open-source image processing and analysis program", https://imagej.nih.gov/ij/index.html (Accessed Jan 30, 2023).

(9) J.J McCann, and V. Vonikakis,. "Calculating Retinal Contrast from Scene Content: A Program", Front. Psychol. | (2018) https://doi.org/10.3389/fpsyg.2017.02079

(10) W.A. Stiehl, J.J. McCann, and R.L.Savoy, (1983). Influence of intraocular scattered light on lightness-scaling experiments. J. Opt. Soc. Am. 73, 1143–1148. doi: 10.1364/JOSA.73.001143

(11) J.J. McCann, (2021b). EdgesGradients. Available at https://www.retinex2.net/Publications/edgesgradients.html (Accessed Jan 30, 2023).

Author Biography

John McCann worked in, and managed, Polaroid's Vision Research Laboratory (1961-1996). He studied Retinex theory, color constancy, color from rod/cone interactions at low light levels, image reproduction, appearance with scattered light, cataracts, and HDR imaging. He is a Fellow of IS&T and the Optical Society of America (OSA); a past President of IS&T, and the Artists Foundation, Boston; IS&T/OSA 2002 Edwin Land Medalist and IS&T 2005 Honorary Member. In 2021 he received the Judd Medal at AIC Judd Medal at their International Congress, Milan.